Shape evolution and shape coexistence in Pt isotopes: comparing interacting boson model configuration mixing and Gogny mean-field energy surfaces

J.E. García-Ramos[1], K. Heyde[2], L.M. Robledo[3], and R. Rodríguez-Guzmán[4,5]
[1]*Departamento de Física Aplicada, Universidad de Huelva, 21071 Huelva, Spain*
[2]*Department of Physics and Astronomy, Ghent University, Proeftuinstraat 86, B-9000 Gent, Belgium*
[2]*Departamento de Física Teórica, Universidad Autónoma de Madrid, 28049 Madrid, Spain*
[4]*Department of Physics and Astronomy, Rice University, Houston, Texas 77005, USA*
[5]*Department of Chemistry, Rice University, Houston, Texas 77005, USA*

The evolution of the total energy surface and the nuclear shape in the isotopic chain $^{172-194}$Pt are studied in the framework of the interacting boson model, including configuration mixing. The results are compared with a self-consistent Hartree-Fock-Bogoliubov calculation using the Gogny-D1S interaction and a good agreement between both approaches shows up. The evolution of the deformation parameters points towards the presence of two different coexisting configurations in the region $176 \leq A \leq 186$.

PACS numbers: 21.10.-k, 21.60.-n, 21.60.Fw.
Keywords: Pt isotopes, shape coexistence, intruder states, Gogny-D1S.

I. INTRODUCTION

Shape coexistence in atomic nuclei has become a very active field of research during the last decades and clear signals of its existence have been obtained at and near proton or neutron closed shells [1–3], more in particular in light nuclei with a closed neutron shell at N = 8, 20, 28 and 40 closed shells as well as in heavy nuclei such as the Sn and the Pb nuclei. It seems that, without exception, shape coexistence is associated with the presence of low-lying excited 0^+ states [1]. The Pb region is a very well-documented example of shape coexistence, both experimental and theoretically (see [1] and references therein). Starting at the neutron closed shell (at N=126), decreasing in mass until reaching the very neutron-deficient nuclei, even going beyond the mid-shell point at N=104, there is ample experimental evidence for shape coexisting bands in both the Pb (Z=82) and Hg (Z=80) nuclei. A question that arises is whether or not this structure, in which two or more bands coexist, survives when moving away from the closed proton shell at Z=82. In particular, the Pt nuclei seem to be a good example to test the survival of the coexisting families of states. It is highly illuminating to compare the systematics of the low-lying states in the energy spectra of the Z=82 proton closed-shell Pb nuclei, the Z=80 Hg nuclei, and the Z=78 Pt nuclei. Whereas the intruder bands are easily singled out for the Pb and Hg nuclei in which the excitation energies display the characteristic parabolic pattern as a function of neutron number N, with a minimal excitation energy around the $N = 104$ neutron mid-shell nucleus, the intruder structure seems "lost" in the Pt nuclei. Focusing on the systematics of the energy spectra in the Pt nuclei, one observes a rather sudden drop in the excitation energy of the 0_2^+, 4_1^+, 2_3^+, and 6_1^+ states between N=110 and N=108, followed by a particularly flat behaviour in excitation energy as a function of neutron number N until the energy of those states start to move up again around neutron number N=100.

To study shape coexistence, there are several approximations available. Among them we have the nuclear shell-model [4] for light nuclei or the selfconsistent mean-field methods for medium and heavy masses mostly of the Hartree-Fock-Bogoliubov (HFB) types [5, 6], as well as their beyond mean-field extensions in the spirit of the Generator Coordinate Method (GCM). In the nuclear shell-model, shape coexistence is obtained by incorporating many-particle many-hole excitations across known closed shells in the model spaces used, while in selfconsistent mean-field methods shape coexistence arises in the form of competing configurations based on different nuclear shapes labelled by the corresponding intrinsic deformations [7–11]. Constrained mean-field calculations are nowdays routinely perfomed with several effective interactions and different levels of sophistication [11, 12]. On the other hand, zero point quantum fluctuations not explicitly considered at the mean-field level can be systematically taken into account within the symmetry-projected GCM [5, 13]. Very recently several works have been carried out in the Pb mass region either starting from Skyrme functional [12, 14–17], using the Gogny interaction [10, 11, 18–22] or the relativistic mean-field (RMF) approach [23–30]. A third alternative comes from a symmetry dictated truncation of the large shell-model space, such as the interacting boson model (IBM) [31]. The IBM starts from the assumption that the low-lying nuclear collective excitations can be described in terms of bosons with angular momentum $L = 0$ (s bosons) and $L = 2$ (d bosons). These building blocks are considered to capture the most important nucleon-nucleon correlations in the formation of nucleon pairs (pairing property and quadrupole collectivity) corresponding to pairs of nucleons either coupled to angular momentum 0 or 2. The number of valence bosons is counted as half the number of valence nucleons, irrespective of their charge (neutrons or protons) or particle/hole character, as shown by Otsuka *et al.* [32].

In the case of the IBM, shape coexistence arises including two-particle two-hole (2p-2h) (or even higher np-nh) excitations across the closed shells, but considering them as extra bosons, *i.e.*, pairs of nucleons. This extension is called IBM configuration mixing (IBM-CM for short) [33]. An advantage of using the IBM is the connection with both the shell-model and the mean-field approach. The extension of the model space in both the nuclear shell-model and the IBM is based on enlarging the model space with multi-particle multi-hole excitations. A drawback of the IBM results from the fact that an increasing number of parameters need to be fitted. They are determined by adjusting to the large body of experimental data, including both excitation energies and B(E2) reduced transition probabilities, using a χ^2 fitting procedure. Thereby, the IBM predictive power becomes curtailed. A possibility to improve the approach is to rely on the ability of the IBM to derive energy surfaces (mean-field energy) associated with a given Hamiltonian [34]. As the mean field parameters are usually adjusted to global properties like binding energies or nuclear matter properties the range of applicability of the mean field extends over the whole periodic table and makes it a good candidate to be used

to fit the parameters defining the IBM Hamiltonian. It is in this spirit that Nomura *et. al.* have recently explored the connection between the IBM Hamiltonian and the mean-field [35], mapping the selfconsistent mean-field energy surfaces onto the IBM space. In the present paper, we exploit the possibility of studying the IBM-CM energy surfaces starting from a Hamiltonian that describes the spectroscopic properties of the chain of isotopes $^{172-194}$Pt. This way to proceed is very different to Nomura's method, because in that case the Hamiltonian's parameters are fixed from the mean-field energy surface, while in the present work from the spectroscopic properties.

In two previous papers [36, 37], we used the IBM-CM to extensively study the Pt nuclei. We carried out a detailed analysis of the energy spectra and absolute B(E2) values for states up to an energy ~ 1.5 MeV. This study allowed us to extract the parameters describing the IBM-CM Hamiltonian in a precise way and we concluded that the presence of intruder configurations does not show up explicitly in the Pt isotopes inspecting the systematics of the experimental data on energy spectra and B(E2) reduced transition probabilities (up to an energy of ~ 1.5 MeV), as compared to the Pb or Hg isotopes. A conclusion was that in the case of the Pt nuclei, the configuration mixing is somehow "hidden". Attempts to describe the $^{172-194}$Pt nuclei without invoking the effect of intruder excitations have been carried out by McCutchan *et al.* [38–40]. In the present paper we will use the parameters given in [36, 37] without any change. Our goal is to study the energy surfaces of $^{172-194}$Pt extracted from phenomenological IBM-CM Hamiltonians, using the intrinsic state formalism including configuration mixing and to compare with selfconsistent mean-field calculations, *i.e.*, a HFB calculation with a Gogny-D1S interaction [11]. A successful comparison, even at a qualitative level, will assess the validity of both viewpoints in the description of shape coexistence.

This particular mass region (including the Pt nuclei) has been also studied in the framework of the IBM by Nomura *et al.* without [41–43] and with the use of configuration mixing [44, 45] using as input the total energy surfaces derived from HFB calculations (Gogny-D1M interaction), with the aim of mapping the mean-field energy surfaces onto IBM energy surfaces and, therefore, to obtain a set of parameters defining the IBM Hamiltonians.

II. THE IBM-CM MODEL

The IBM-CM allows the simultaneous treatment and mixing of several boson configurations which correspond to different particle–hole (p–h) shell-model excitations [33]. In the approach that is used in the present study no distinction is made between particle- and hole-bosons. Thus, the Hamiltonian describing the interacting system of two configurations, one called the "regular" configuration, corresponding to N bosons and the other called the "intruder" configuration, corresponding to N+2 bosons, including the mixing term between the [N] and [N+2] boson systems, can be written as

$$\hat{H} = \hat{P}_N^\dagger \hat{H}^N_{\rm ecqf} \hat{P}_N + \hat{P}^\dagger_{N+2} \left(\hat{H}^{N+2}_{\rm ecqf} + \Delta^{N+2} \right) \hat{P}_{N+2} \ + \hat{V}^{N,N+2}_{\rm mix} \ , \tag{1}$$

where $\hat{P}_N$ and $\hat{P}_{N+2}$ are projection operators onto the $[N]$ and the $[N+2]$ boson spaces respectively, $\hat{V}^{N,N+2}_{\rm mix}$ describes the mixing between the $[N]$ and the $[N+2]$ boson subspaces, and

$$\hat{H}^i_{\rm ecqf} = \varepsilon_i \hat{n}_d + \kappa'_i \hat{L} \cdot \hat{L} + \kappa_i \hat{Q}(\chi_i) \cdot \hat{Q}(\chi_i), \tag{2}$$

is the extended consistent-Q Hamiltonian (ECQF) [46], with $i = N, N+2$, $\hat{n}_d$ the d boson number operator,

$$\hat{L}_\mu = [d^\dagger \times \tilde{d}]^{(1)}_\mu, \tag{3}$$

the angular momentum operator, and

$$\hat{Q}_\mu(\chi_i) = [s^\dagger \times \tilde{d} + d^\dagger \times s]^{(2)}_\mu + \chi_i [d^\dagger \times \tilde{d}]^{(2)}_\mu \ , \tag{4}$$

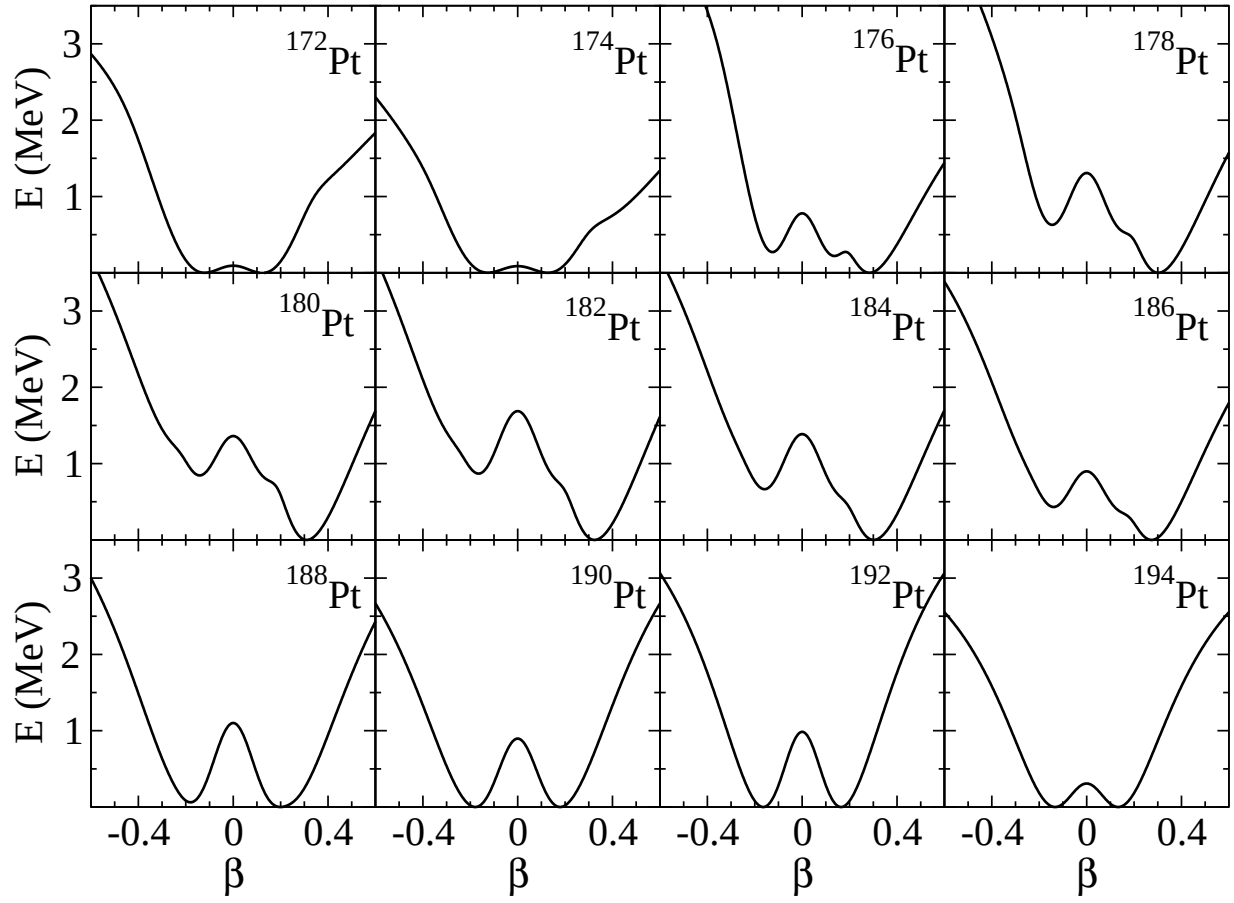

FIG. 1: IBM-CM total energy curves for $^{172-194}$Pt as a function of the β deformation parameter (IBM-CM parameters as given in [36]).

the quadrupole operator.

The parameter Δ^{N+2} can be associated with the energy needed to excite two particles across the $Z = 82$ shell gap, corrected for the pairing interaction energy gain and including monopole effects [47, 48]. The operator $\hat{V}_{\rm mix}^{N,N+2}$ describes the mixing between the $[N]$ and the $[N+2]$ configurations and is defined as

$$\hat{V}_{\rm mix}^{N,N+2} = w_0^{N,N+2}(s^\dagger \times s^\dagger + s \times s) + w_2^{N,N+2}(d^\dagger \times d^\dagger + \tilde{d} \times \tilde{d})^{(0)}. \quad (5)$$

The considered Hamiltonian is not the most general one in each Hilbert space, [N] and [N+2], but this approach has been shown to be a rather good approximation in many realistic calculations [31]. In particular, in the present study, we have taken the parameters obtained in [36].

These parameters are quite different from the ones obtained by Nomura *et al.* in [41] mostly due to the following reasons: First, the present IBM-CM makes no distinction between proton and neutron bosons, while [41] do not use configuration mixing but take into account the distinction between protons and neutrons, *i.e.*, they use IBM-2 [31]. Second, we obtain the Hamiltonian's parameters directly from experimental spectroscopic properties, while in [41] the authors extract them from a selfconsistent mean-field energy surface, through a mapping procedure.

III. ENERGY SURFACES

In the eighty's a geometric interpretation of the IBM was proposed by Ginocchio and Kirson [34], using the so-called intrinsic state formalism. To define the intrinsic state, one assumes that the dynamical behavior of the system can be described using independent bosons moving in an average field. The ground state of the system is a condensate $|N; \beta_B, \gamma_B\rangle$ of bosons (the B subindex stands for boson, as used in Ref. [35]), occupying the lowest-energy phonon

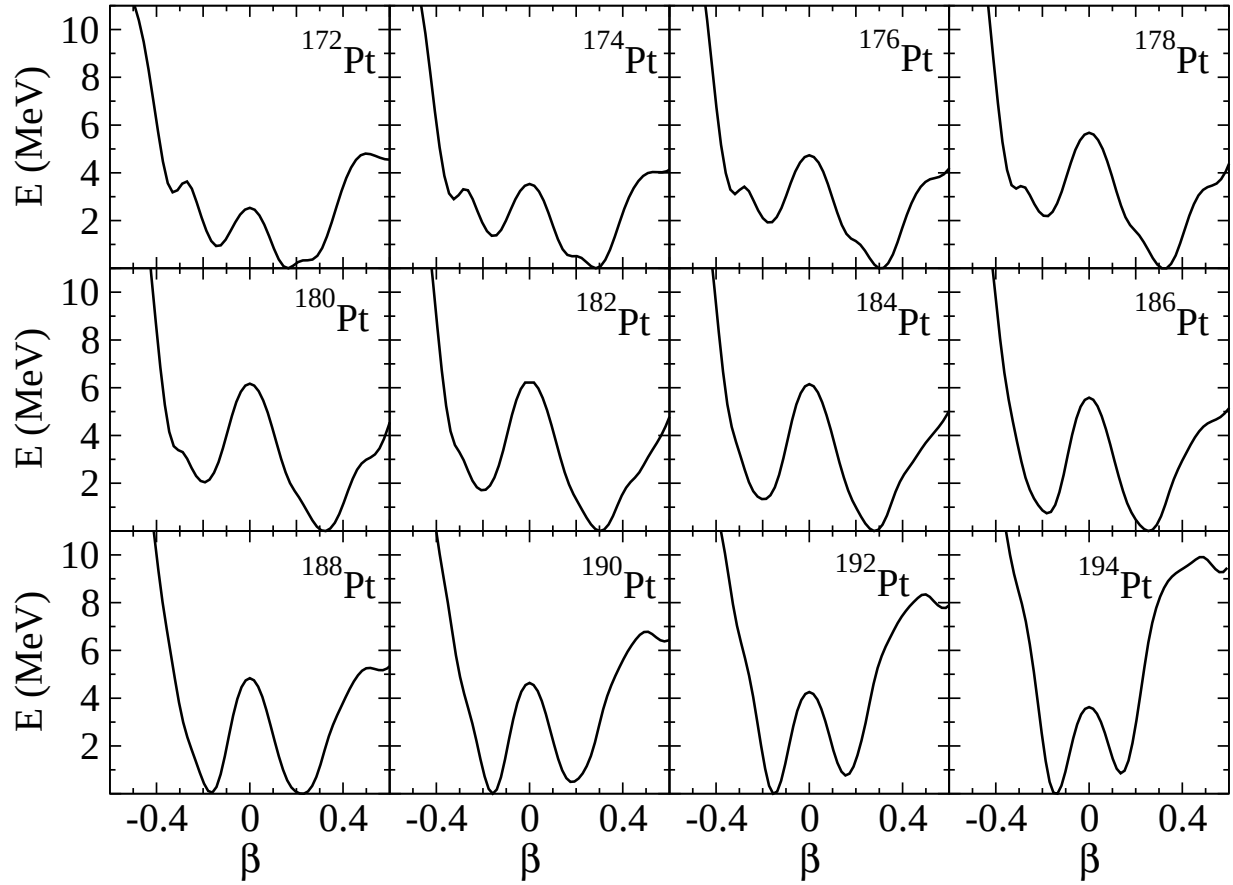

FIG. 2: Hartree-Fock-Bogoliubov total energy curves for $^{172-194}$Pt as a function of the axial quadrupole deformation parameter β (see also Ref. [11]).

state, $\Gamma_c^\dagger$,

$$|N;\beta_B,\gamma_B\rangle = \frac{1}{\sqrt{N!}}(\Gamma_c^\dagger)^N|0\rangle, \tag{6}$$

where

$$\Gamma_c^\dagger = \frac{1}{\sqrt{1+\beta_B^2}}\left(s^\dagger + \beta_B\cos\gamma_B\, d_0^\dagger + \frac{1}{\sqrt{2}}\beta_B\sin\gamma_B\,(d_2^\dagger + d_{-2}^\dagger)\right), \tag{7}$$

$d_\mu^\dagger$ corresponds to the μ component of the $d^\dagger$ operator and β_B and γ_B are variational parameters related with the shape variables in the geometrical collective model [49], and the reference boson vacuum state, containing no s nor d bosons is denoted by the ket vector $|0\rangle$. The expectation value of the Hamiltonian in the intrinsic state (6) provides the energy surface of the system, $E(N,\beta_B,\gamma_B) = \langle N;\beta_B,\gamma_B|\hat{H}|N;\beta_B,\gamma_B\rangle$. The values of β_B and γ_B which minimize the expectation value of the energy, *i.e.*, the equilibrium values, provide the shape of the nucleus.

The extension of the IBM geometrical picture in order to include configuration mixing was proposed by Frank *et al.* [50–53] by means of a matrix coherent-state method that allows to describe shape coexistence phenomena. The way to proceed is to define a model space with states $|N;\beta_B,\gamma_B\rangle$, $|\,N+2;\beta_B,\gamma_B\rangle$ and to diagonalize the Hamiltonian (1). Therefore, one needs to construct the 2×2 matrix:

$$H_{CM} = \begin{pmatrix} E(N,\beta_B,\gamma_B) & \Omega(\beta_B) \\ \Omega(\beta_B) & E(N+2,\beta_B,\gamma_B) \end{pmatrix}. \tag{8}$$

The diagonal terms $E(N,\beta_B,\gamma_B)$ and $E(N+2,\beta_B,\gamma_B)$ only contain the N and the $N+2$ contributions of the Hamiltonian (1), respectively, while $\Omega(\beta_B)$ corresponds to the matrix element describing the mixing of the $[N]$ and

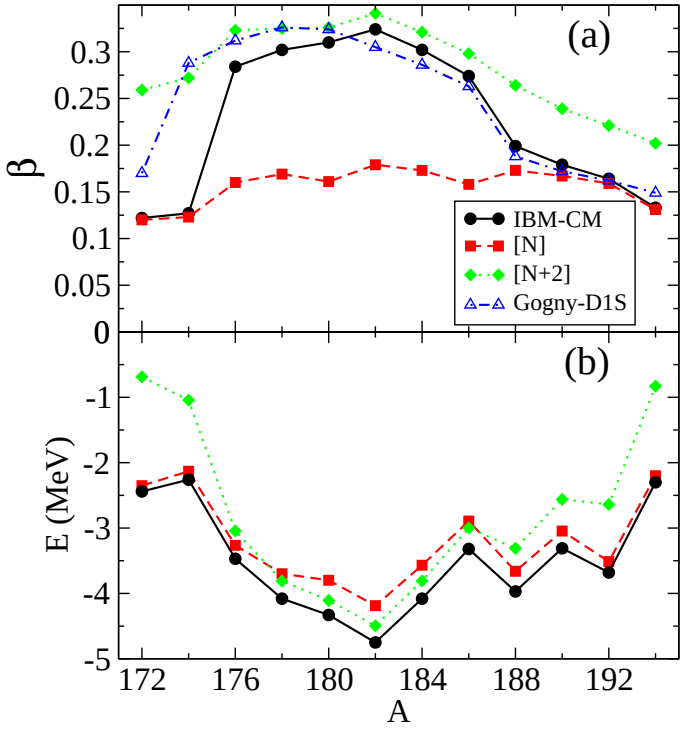

FIG. 3: (Color online) (a): Comparison of the value of β for IBM-CM and for selfconsistent HFB. We also plot the value of β corresponding with the unperturbed "regular", $[N]$, and the unperturbed "intruder", $[N+2]$, configurations. (b): energy of the unperturbed regular and intruder IBM bandheads, compared with the ground state energy (full IBM-CM diagonalization).

$[N+2]$ configurations. The expressions for both the diagonal and non-diagonal matrix elements (see Ref. [53]) are:

$$E_i(N_i,\beta_B,\gamma_B) = (\varepsilon_i+6\kappa_i')\frac{N_i\beta_B^2}{1+\beta_B^2}+\kappa_i\left(\frac{N_i}{1+\beta_B^2}(5+(1+\chi_i^2)\beta_B^2)+\frac{N_i(N_i-1)}{(1+\beta_B^2)^2}\right.$$
$$\left.\times\ (\frac{2}{7}\chi_i^2\beta_B^4-4\sqrt{\frac{2}{7}}\chi_i\beta_B^3\cos 3\gamma_B+4\beta_B^2)\right), \quad (9)$$

$$\Omega(\beta_B) = \frac{\sqrt{(N_i+2)(N_i+1)}}{1+\beta_B^2}\left(w_0^{N,N+2}+w_2^{N,N+2}\frac{\beta_B^2}{\sqrt{5}}\right). \quad (10)$$

To obtain the energy surface one has to diagonalize (8) and to consider the lowest eigenvalue.

In the present study, with the aim to obtain the corresponding mean-field surfaces for the considered nuclei, we have resorted to the HFB [6] approximation based on the parametrization D1S of the Gogny interaction [11]. In the calculation of the total energy surfaces for the Pt nuclei [11], the HFB quasiparticle operators have been expanded in a harmonic oscillator basis containing enough shells (N_{shell}=13 major shells in the present case) in order to guarantee convergence for all values of the mass quadrupole operator and for all the Pt isotopes. In order to construct the total energy contour plots in the $(\beta-\gamma)$ plane, we have to constrain the different components of the quadrupole operator:

$$Q_{20} = \frac{1}{2}\langle\Phi_{HFB}|2z^2-x^2-y^2|\Phi_{HFB}\rangle, \quad (11)$$

$$Q_{22} = \frac{\sqrt{3}}{2}\langle\Phi_{HFB}|x^2-y^2|\Phi_{HFB}\rangle, \quad (12)$$

$$Q = \sqrt{Q_{20}^2+Q_{22}^2}, \quad (13)$$

$$\tan\gamma = \frac{Q_{22}}{Q_{20}}. \tag{14}$$

The relationship between Q and β can be found in [49] and results to be,

$$\beta = \sqrt{\frac{4\pi}{5}}\frac{Q}{A\langle r^2\rangle}, \tag{15}$$

where $\langle r^2\rangle = 3/5 r_0^2 A^{2/3}$ ($r_0 = 1.2$ fm). Further details can be found in [54].

To compare IBM-CM and HFB total energy surfaces one needs to establish a relationship between (β_B, γ_B) and (β, γ). This problem was first studied by Ginocchio and Kirson [34] with as a result that $\gamma_B = \gamma$ and the semi-quantitative relationship,

$$\beta \leq 1.18\frac{2N}{A}\beta_B. \tag{16}$$

The latter provides the functional dependence between β and β_B and establishes that β is much smaller than β_B, however the precise mapping is an involved task. Moreover, expression (16) should be modified because of the presence of two different configurations with different number of active bosons, N and $N+2$, respectively. Extending Eq. (16) to the IBM-CM approach, one should sum up the contributions from both configurations weighted with the square of the amplitude of the wave function in the N space, ω (see [36, 37]),

$$\beta = 1.18\frac{2}{A}\beta_B(N + 2\ (1-\omega)). \tag{17}$$

Comparing the value of β resulting from both approaches one cannot expect an exact agreement (according to [34] "we should not take the actual numerical values (of β) too seriously"). To improve the results we will use as an *ansatz*,

$$\beta = 1.18\frac{2}{A}\beta_B(N + 2\ (1-\omega))\ \delta + \xi. \tag{18}$$

We have performed a least-squares fit between the IBM and HFB β equilibrium values, obtaining $\delta = 1.37$ and $\xi = 0.07$. In section IV all the results presented for the IBM-CM make use of the above scale transformation (18). In [35], the authors established the connection between β_B and β through a mapping procedure among the mean-field and the IBM energy surfaces.

IV. RESULTS AND DISCUSSION

In Fig. 1, we show for every Pt isotope (covering the mass interval $172 \leq A \leq 194$) the IBM-CM energy curves along the axial symmetry axis, as a function of the deformation parameter, β. Prolate shapes correspond to $\beta > 0$ while oblate shapes to $\beta < 0$. These curves correspond to the lowest eigenvalue of the matrix (8). The lightest isotopes, $^{172-174}$Pt, present two very shallow degenerate minima, oblate and prolate, respectively, that correspond to a small value of β, with a rather modest barrier at $\beta = 0$. Consequently, in the present approach, these isotopes are close to exhibiting a spherical shape. The next isotope, ^{176}Pt, starts to develop a more pronounced deformed minimum. Indeed two prolate and an oblate minimum are observed for this isotope, the deeper minimum corresponding to the more deformed minimum with $\beta \approx 0.3$. The $^{178-186}$Pt isotopes show a similar structure, with a well-deformed prolate minimum, $\beta \approx 0.3$, a large barrier at $\beta = 0$, of about 1.5 MeV, and an oblate local minimum. Finally, the $^{188-194}$Pt isotopes exhibit two quasi-degenerate minima, at the same value of β, the first prolate while the second oblate, with an equilibrium value of β which decreases from $\beta \approx 0.2$ for ^{188}Pt towards $\beta \approx 0.13$ in ^{194}Pt. The height of the central barrier remains almost constant for $^{188-192}$Pt at a value ≈ 1 MeV, but is strongly reduced to 0.3 MeV in ^{194}Pt.

In order to carry out a comparison with the selfconsistent mean-field HFB calculations using the Gogny-D1S interaction, we show in Fig. 2 the energy curves along the axial symmetry axis (see also Fig. 1 of Ref. [11]) for the same set of Pt isotopes as shown in Fig. 1. The lightest isotope ^{172}Pt shows a prolate deformed ground state with $\beta \approx 0.17$, though less deformed than its neighbours, and also presents an oblate local minimum (see Fig. 5). The isotopes $^{174-184}$Pt present a rather similar structure with a deep prolate minimum at $\beta \approx 0.3$ and an oblate local minimum. They display a large spherical barrier whose height increases from 3.5 MeV in ^{174}Pt to more than 6 MeV in ^{182}Pt. For these isotopes, we also observe a reduction in the excitation energy of the oblate local minimum point with respect to the prolate ground state. On the other hand the spherical barrier starts to decrease and the prolate

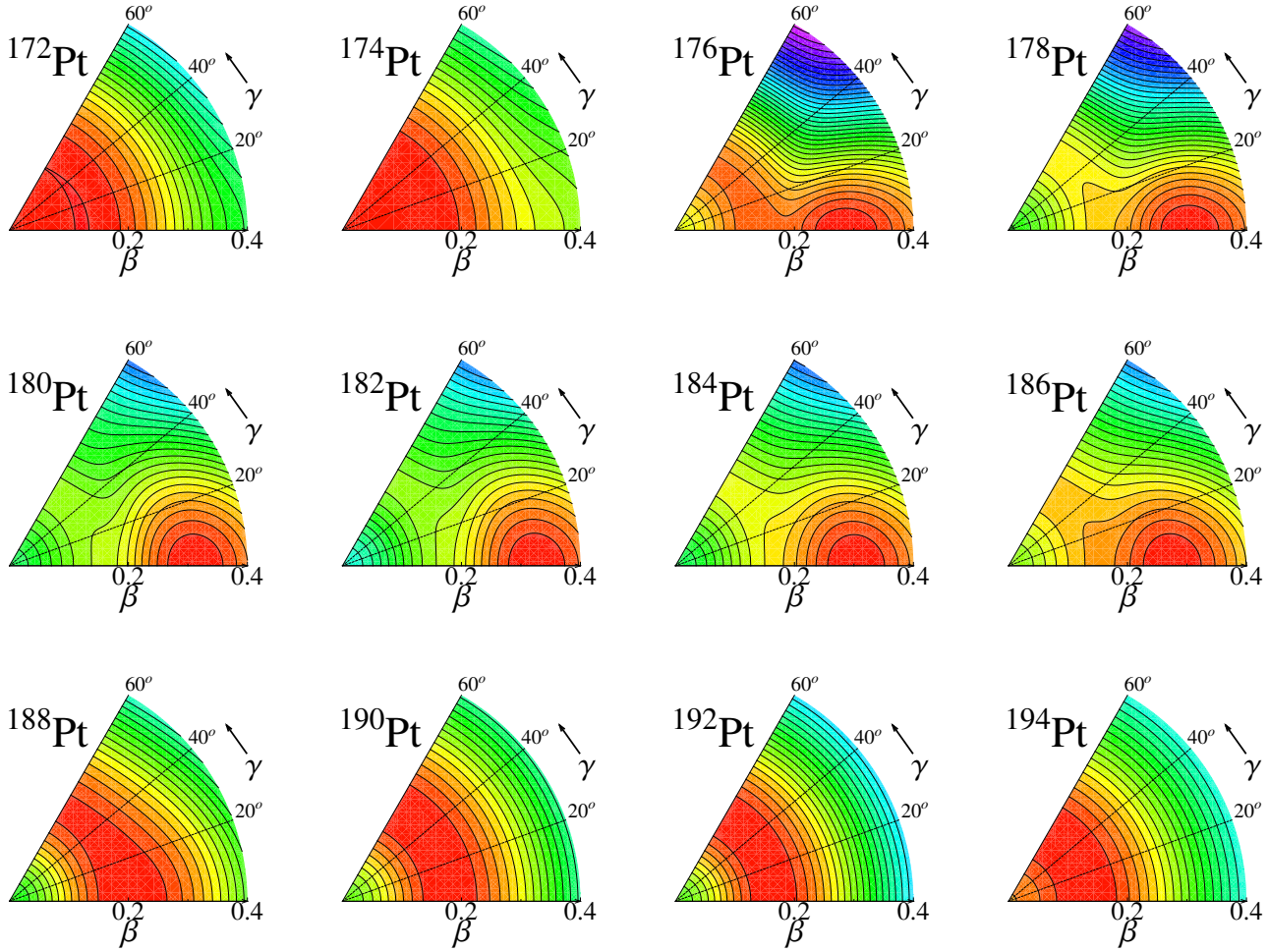

FIG. 4: (Color online) IBM-CM contour plots for $^{172-194}$Pt as a function of β and γ (IBM-CM parameters as given in [36]). The separation between adjacent contour lines amounts to 100 keV. The deepest energy minimum is set to zero, corresponding to the red color, while green corresponds to ≈ 3 MeV.

and oblate axial minima become almost degenerate, in particular for ^{188}Pt. From this isotope onwards the ground state turns out to be oblate while the prolate minimum lies higher in energy. Finally, the height of the spherical barrier steadily decreases and the equilibrium value of β changes from ≈ 0.2 in ^{188}Pt to ≈ 0.13 in ^{194}Pt.

Comparing both approaches, (i) we first of all notice a different energy scale, in particular regarding the height of the spherical barrier. In the case of the IBM-CM, this height amounts for ≈ 1.8 MeV in the largest case, while in the mean-field HFB approach, this energy becomes as large as 6 MeV, (ii) on the other hand, the onset of deformation does not happen precisely at the same masses. In particular, $^{172-174}$Pt appear to be almost spherical in the IBM-CM calculations, while in the mean-field HFB calculations, a well deformed shape is obtained, (iii) in spite of the previous differences, the similarity between both approaches is remarkable for $^{176-188}$Pt, for which the spherical barrier heights (up to an energy scale), the prolate-oblate energy differences, and the position of the corresponding minima agree reasonably well. We remark that for ^{188}Pt, both approaches result in degenerate prolate and oblate minima. Finally, for $^{190-194}$Pt the IBM produces prolate and oblate minima that are degenerate, while mean-field HFB calculations indicate an oblate minimum, even though the prolate-oblate energy difference is quite small all the time. It is worth noticing that serious differences result between both approaches concerning the energy scale. A similar situation is observed by Kotila *et al.* [55] where selfconsistent HF+BCS, mapped IBM, and phenomenological IBM energy surfaces are compared. The first two present a much larger energy scale as compared with the phenomenolocical IBM energy surface, which has been obtained from a fit to the experimental excitation energies and B(E2) transitions rates. Therefore, these two cases point towards the existence of quite different energy scales resulting from the microscopic and phenomenological calculations.

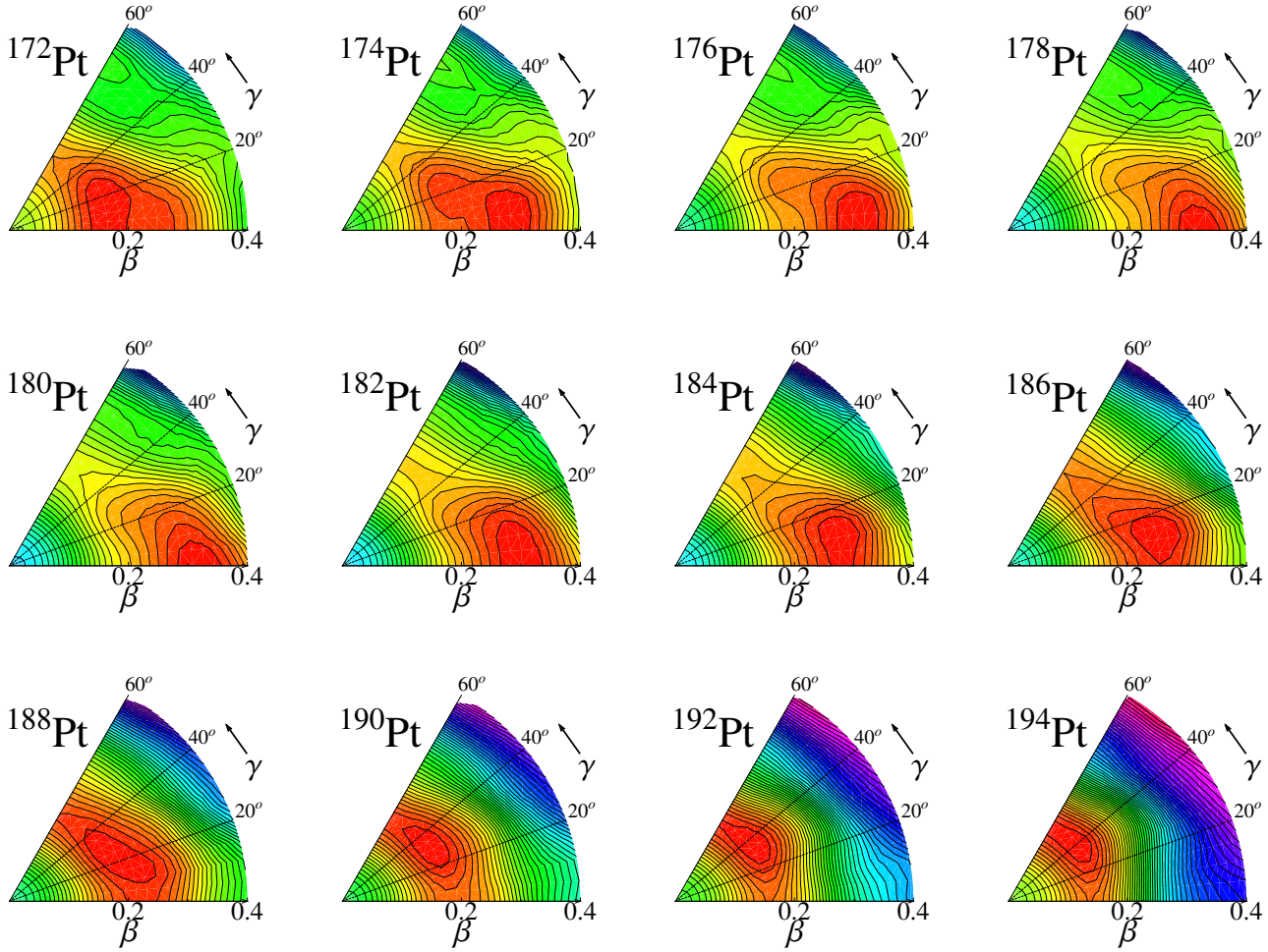

FIG. 5: (Color online) Hartree-Fock-Bogoliubov contour plots for $^{172-194}$Pt as a function of β and γ (see also Ref. [11]). The separation between adjacent contour lines amounts to 250 keV and the deepest energy minimum is set to zero, corresponding to the red color, while green corresponds to $\approx$ 10 MeV.

A very convenient way to compare the overall outcome of both approaches is to plot the value of β of the IBM-CM with the one of HFB as a function of the mass number. In Fig. 3 (a) we depict the β deformation parameter provided by the IBM-CM and the one obtained within the Gogny-D1S HFB framework. In additon, in the same panel (a), we also plot the β value corresponding to the unperturbed regular $[N]$ and the intruder $[N+2]$ configurations as "reference" values (see also Ref. [56]). As can be seen, there is an overall agreement between the mean-field HFB and the IBM approaches. Both approaches point towards large values of the deformation β around neutron mid shell, though the precise neutron number where a sudden onset of deformation arises is different in both cases: the nucleus ^{174}Pt for the HFB calculation and ^{176}Pt for the IBM-CM calculation, respectively. In Fig. 3 (b), we plot the IBM-CM bandhead energy for both unperturbed structures besides the value of the ground-state energy (full IBM-CM calculation). Note that these unperturbed energies correspond to the diagonalization of the IBM Hamiltonian. Analyzing these energy curves, one observes a crossing at $^{176-178}$Pt and at $^{186-188}$Pt. These points delimit the area where the intruder configuration becomes the ground state. Taking into account that the intruder configuration corresponds to a more deformed shape than the regular one (see the unperturbed curves in the top panel), it becomes evident why the Pt isotopes around the mid-shell N=104 (A=182) are more deformed. In the mean-field approximation, deformation results from the spontaneous breaking of the rotational symmetry [11, 54] in the considered nuclei. It is quite remarkable that only one symmetry-broken mean-field configuration already accounts for the trend that is otherwise only obtained within the IBM-CM by invoking the [N+2] intruder configurations. On the other hand, we see how both approximations are complementary with the IBM-CM providing an intuitive geometrical picture for the onset of deformation around the neutron mid-shell.

Even though the calculations along the β axis (only considering the axially symmetric shapes) already give a clear view of the shape evolution, it is the calculation in the full $(\beta-\gamma)$ plane which provides the more realistic "image" of the nuclear shape. Indeed, we will see that for the heaviest Pt isotopes the triaxial degree of freedom, γ, plays a notable role [11].

Before starting with he analysis of the Pt $(\beta-\gamma)$ total energy contour plots, it is worth to mention some characteristics of the IBM-CM parameterization. In order to determine the IBM parameters, as described in [36], we imposed a number of constraints to reduce the number of free parameters. In particular, we have considered ε_{N+2} as well as χ_N to be equal to zero for the whole isotopic chain. This latter constraint has an immediate consequence on the energy surfaces, *i.e.*, whenever the regular configuration describes the ground state of a given Pt nucleus, the resulting energy surface will be flat in the γ direction, or, γ unstable. Therefore, in the present IBM-CM approach, the possibility to generate triaxiallity or oblate shapes is absent. In the standard IBM the triaxiallity is easily accommodated through the inclusion of three-body terms in the Hamiltonian [57, 58]. In IBM-2 [31] and IBM-CM triaxiallity can be generated with two orthogonal ellipsoids for protons and neutrons [59] and with the mixing of two configurations with different prolate/oblate character [60], respectively. Nomura *et al.* [45, 61] have shown that including a three-boson interaction within the IBM-2 formulation, treating proton and neutron bosons explicitely, naturally leads to cover the full $(\beta-\gamma)$ plane. This turns out not to form a major drawback of the present IBM-CM approach when comparing with the mean-field HFB energy surfaces for the Pt isotopes. The reason being, as discussed later, that the heaviest isotopes, though oblate in the mean-field HFB approach, are not very far removed from being γ unstable.

In Fig. 4 we depict the IBM-CM energy surfaces for the chain of isotopes $^{172-194}$Pt. In $^{172-174}$Pt, we observe a flat minimum at $\beta = 0$, which indeed corresponds to a slightly deformed γ-unstable minimum as was observed in the corresponding axial energy plot (see Fig. 1). In the nucleus ^{176}Pt, one observes the onset of a more deformed minimum, resulting in the coexistence of a γ-unstable and a prolate deformed minimum. This isotope is the only in which two minima coexist. In $^{178-186}$Pt the isotopes present a well-pronounced prolate minimum around $\beta = 0.3$. Finally the nuclei $^{188-194}$Pt become less deformed than the medium-mass isotopes and turn out to be γ-unstable. Note that in the present IBM-CM approach, no genuine triaxial shapes can appear for the Pt isotopes, although, as mentioned before, triaxiallity can be generated through the use of more general Hamiltonians.

In Fig. 5 we present the energy contour plots computed with the Gogny-D1S interaction for the isotopes $^{172-194}$Pt (see also Fig. 2 of Ref. [11]). In this case, the nuclei $^{172-174}$Pt have a slightly triaxial shape. On the other hand, the isotope ^{176}Pt appears as more deformed than the lighter ones with a prolate shape. Prolate deformed shapes are also predicted for $^{178-182}$Pt while a triaxial shape develops in $^{184-190}$Pt. In particular, for ^{190}Pt the shape corresponds to $\gamma \approx 30^\circ$. Finally, $^{192-194}$Pt still present triaxial shapes but the heavier isotopes come close to exhibit an oblate shape.

In summary, in the IBM-CM approach, the lightest Pt isotopes, *i.e.*, $^{172-174}$Pt, are slightly deformed. In ^{176}Pt a prolate and a γ-unstable minimum coexist, but quickly, a well deformed prolate minimum develops in ^{178}Pt, becoming the most pronounced prolate minimum at the mid-shell, *i.e.*, in ^{182}Pt with the prolate shape remaining well pronounced up to ^{186}Pt. Moving towards heavier mass Pt isotopes, γ-flat energy surfaces start to develop. Indeed, for ^{188}Pt, a very extended energy surface develops in the γ direction, becoming completely γ-unstable when reaching $^{190-194}$Pt. For the set of IBM-CM parameters used in this work no genuine triaxial shapes can be generated although this can be done using three-body terms in the Hamiltonian, having orthogonal proton and neutron ellipsoids in IBM-2 or mixing configurations with different prolate/oblate character in IBM-CM. In the mean-field HFB approach, the lightest Pt isotopes are slightly prolate. Moving to the larger masses, the Pt isotopes become more deformed, but at the same time the total energy surface starts to flatten in the γ direction. Passing mid-shell (at N = 104, A = 182), the nuclei become triaxial and the heaviest Pt isotopes already correspond to oblate shapes. Therefore, the evolution of the IBM-CM energy surfaces correspond, to a large extent, with the corresponding total energy surfaces obtained from a mean-field HFB approach. The most pronounced difference appears for the heaviest Pt isotopes, in which the mean-field HFB approach results in triaxial shapes while the IBM-CM parameterization results in γ-unstable shapes.

A similar analysis was carried out by Morales *et al.* [53] for the even-even Pt nuclei from $A = 182$ up to $A = 204$. They started from the set of IBM parameters obtained in the schematic study of Harder *et al.* [62]. The latter study was performed with the aim of providing a schematic description of the $^{182-204}$Pt energy spectrum and, indeed, the agreement with the experimental excitation energies is only qualitative. In Ref. [53] it was shown that the absolute minimum in the energy surface evolves from a prolate into an oblate shape, finally turning into a spherical shape with increasing neutron number, starting at $N = 104$ and ending at the closed shell value of $N = 126$. Indications for shape coexistence result in the isotopes $^{182-188}$Pt. A comparison with the results we derive from the present IBM-CM Hamiltonian gives an idea about the sensitivity of the energy variations in the IBM parameters.

It is also interesting to compare the present IBM-CM energy surfaces with the ones resulting from the mapping of the selfconsistent mean-field HFB calculations carried out by Nomura *et al.* [41]. In this latter case, the extracted IBM energy surfaces match very well with the HFB results by obvious reasons and, therefore, reproduce the shape evolution from a prolate to an oblate shape passing through a triaxial region. This is expected because the mapped

Hamiltonian was determined through a mapping of the HFB total energy surfaces as closely as possible onto the corresponding IBM mean-field surfaces. The agreement between both IBM approaches is reasonable, but once more a large difference in the energy scale (heigth of the spherical barrier) between is observed. The origin of this difference deserves further investigation.

Finally, it is also of interest to compare with previous phenomenological mean-field studies. Calculations by Bengtsson *et al.* [7], starting from a deformed Woods-Saxon potential, show that the energy surfaces obtained for the Pt nuclei turn out to exhibit a more complex behavior when comparing with results obtained for the Hg nuclei, covering the region $98 \leq N \leq 120$ region. The prolate minimum is lowest in the mass interval $178 \leq A \leq 186$, whereas the oblate minimum becomes lowest for $A = 192$ and onwards to heavier Pt nuclei. The transition at $A = 188, 190$ and, at the lower mass side, at $A = 176$, passes through a γ-soft energy surface. Hilberath *et al.* [63], who calculated total Routhian surfaces also using a deformed Woods-Saxon potential, arrive at very much the same results. Both of these results are largely consistent with the present IBM-CM matrix coherent-state mean-field results discussed before. Furthermore, calculations within the framework of the relativistic mean-field approximation have been carried out by Fossion *et al.* [27] for the Pt nuclei in the mass region $184 \leq A \leq 202$. The results point out towards a transition from a prolate, as the lowest one in $A = 186$, towards an oblate minimum, as the lowest one in $A = 188$, with both minima present in the region $184 \leq A \leq 192$. Beyond ^{194}Pt, the energy surface becomes rather flat, evolving towards a spherical minimum at ^{200}Pt and beyond. The possibility of triaxial deformation was not considered.

V. SUMMARY

In summary we have carried out a detailed comparison of nuclear total energy surfaces obtained using two approaches: the IBM-CM, formulated within a laboratory frame, and the selfconsistent mean-field HFB approach, starting from the Gogny-D1S interaction, which is an intrinsic frame formulation. The total energy surfaces resulting from both approaches are qualitatively similar even though they have totally different starting point. The first one is a more phenomenological approach in which the parameters that determine the IBM-CM Hamiltonian and, consequently also define the resulting energy surfaces, are obtained making a careful comparison between the large set of spectroscopic properties and the corresponding theoretical results. The second approach is a mean-field one based on the Gogny-D1S effective interaction whose predicted power all over the nuclear chart has been shown in previous studies both at the mean-field level and beyond [11]. Both approaches result in a consistent description of the nuclear energy landscape which is at the origin of shape evolution in the Pt isotopes. The common results point towards the fact that the lightest Pt isotopes are slightly deformed and prolate, becoming more strongly deformed shapes, while at the same time the potential in the γ direction starts to flatten, developing a triaxial shape once having passed mid shell (at N=104, A=182) and finally becoming oblate for $^{192-194}$Pt (γ-unstable in the IBM-CM case).

Even though total energy surfaces from the above approaches are very similar in structure for the Pt nuclei discussed in the present paper, the final comparison between these approaches has, of course, to be made at the level of the nuclear observables: energy spectra, electromagnetic properties, ground-state properties (charge radii), ... The IBM, being an algebraic model, has an intrinsic geometric structure related to the particular Hamiltonian used. As discussed in Sect. III, and amply illustrated in the present paper, the crucial ingredient is the use of coherent states resulting in energy surfaces that can be compared with the results calculated using a selfconsistent mean-field HFB approach, starting from a microscopic basis. It is most interesting to observe a very similar overall description of the energy surfaces describing the long series of Pt isotopes. A next step in comparing both approaches will be situated on the level of beyond mean-field calculations (BMF), that allow for the calculation of energy spectra, electromagnetic properties, ..., which should be compared with the results obtained from the IBM-CM calculations. In this way, the effect of the collective inertia, inherent to the GCM, will be explicitly taken into account. Comparing a large set of observables, as outlined before, obtained from a BMF calculation using the Gogny interaction, with the corresponding observables calculated using the mapped IBM Hamiltonian [35] will form a major step in order to understand the connection between both approaches. This could be a topic of further study.

VI. ACKNOWLEDGEMENTS

We thank M. Huyse, P. Van Duppen for continuous interest in this research topic and J.L. Wood for stimulating discussions in various stages of this work. Financial support from the "FWO-Vlaanderen" (KH and JEGR) and the InterUniversity Attraction Poles Programme - Belgian State - Federal Office for Scientific, Technical and Cultural Affairs (IAP Grant No. P7/12, is acknowledged. This work has also been partially supported by the Spanish Ministerio de Economía y Competitividad and the European regional development fund (FEDER) under Project Nos.

FIS2011-28738-C02-02, FPA2012-34694, FIS2012-34479 and by Junta de Andalucía under Project No. FQM318, and P07-FQM-02962, as well as by Spanish Consolider-Ingenio 2010 (CPANCSD2007-00042).

[1] K. Heyde and J.L. Wood, Revs. Mod. Phys. **83**, 1467 (2011).
[2] K. Heyde, P. Van Isacker, M. Waroquier, J.L. Wood, and R.A. Meyer, Phys. Rep. **102**, 291 (1983).
[3] J.L. Wood, K. Heyde, W. Nazarewicz, M. Huyse, and P. Van Duppen, Phys. Rep. **215**, 101 (1992).
[4] E. Caurier and G. Martínez-Pinedo and F. Nowacki and A. Poves and A. P. Zuker, Rev. Mod. Phys. **77**, 427 2005.
[5] M. Bender, P.-H. Heenen, and P.-G. Reinhard, Rev. Mod. Phys. **75**, 121 (2003).
[6] P. Ring and P. Shuck, *The nuclear many-body problem*, Springer-Verlag (1980).
[7] R. Bengtsson, T. Bengtsson, J. Dudek, G. Leander, W. Nazarewicz, and Jing-Ye Zhang, Phys. Lett. **B 183**, 1 (1987).
[8] R. Bengtsson and W. Nazarewicz, Z. Phys. **A 334**, 269 (1989).
[9] W. Nazarewicz, Phys. Lett. **B 305**, 195 (1993).
[10] J.L. Egido, L.M. Robledo, and R.R. Rodríguez-Guzmán, Phys. Rev. Lett. **93**, 082502 (2004).
[11] R. Rodríguez-Guzmán, P. Sarriguren, L.M. Robledo, and J.E. García-Ramos, Phys. Rev. **C 81**, 024310 (2010).
[12] T. Duguet, M. Bender, P. Bonche, and P.-H. Heenen, Phys. Lett. **B 559**, 201 (2003).
[13] R. Rodríguez-Guzmán, L. Egido, and L.M. Robledo, Nucl. Phys. **A 709**, 201 (2002).
[14] N.A. Smirnova, P.-H. Heenen, and G. Neyens, Phys. Lett. **B 569**, 151 (2003).
[15] M. Bender, P. Bonche, T. Duguet, and P.-H. Heenen, Phys. Rev. **C 69**, 064303 (2004).
[16] T. Grahn *et al.*, Nucl. Phys.**A 801**, 83 (2008).
[17] J.M. Yao, M. Bender, and P.-H. Heenen, Phys. Rev. **C 87**, 034322 (2013).
[18] M. Girod, J.P. Delaroche, D. Gogny, and J.F. Berger, Phys. Rev. Lett. **62**, 2452 (1989).
[19] J. P. Delaroche *et al.*, Phys. Rev. **C 50**, 2332 (1994).
[20] R.R. Chasman, J.L. Egido, and L.M. Robledo, Phys. Lett. **B 513**, 325 (2001).
[21] R.R. Rodríguez-Guzmán, J.L Egido, and L.M. Robledo, Phys. Rev. **C 69**, 054319 (2004).
[22] P. Sarriguren, R. Rodríguez-Guzmán, and L.M. Robledo, Phys. Rev. **C 77**, 064322 (2008).
[23] M. M. Sharma, and P. Ring, Phys. Rev. **46**, 1715 (1992).
[24] S.K. Patra, S. Yoshida, N. Takigawa, and C.R. Praharaj, Phys. Rev. **C 50**, 1924 (1994).
[25] S. Yoshida, S. K. Patra, N. Takigawa, and C.R. Praharaj, Rev. **C 50**, 1924 (1994).
[26] S. Yoshida, and N. Takigawa, Phys. Rev. **C 55**, 1255 (1997).
[27] R. Fossion, D. Bonatsos, and G.A. Lalazissis, Phys. Rev. **C 73**, 044310 (2006).
[28] T. Nikšić, D. Vretenar, P. Ring, andd G. A. Lalazissis. Phys. Rev. **65**, 054320 (2002).
[29] T. Nikšić, P. Ring, D. Vretenar, Y. Tian, and Z.Y Ma, Phys. Rev. **C 81**, 054318 (2010).
[30] T. Nikšić, D. Vretenar, and P. Ring, Progr. Part. Nucl. Phys. **66**, 519 (2011).
[31] F. Iachello and A. Arima, *The Interacting Boson Model*, Cambridge University Press (1987).
[32] T. Otsuka, A. Arima, and F. Iachello, Nucl. Phys. **A 309**, 1 (1978).
[33] P.D. Duval and B.R. Barrett, Nucl. Phys. **A 376**, 213 (1982).
[34] J.N. Ginocchio and M.W. Kirson, Nucl. Phys. **A 350**, 31, (1980); A.E.L. Dieperink and O. Scholten, Nucl. Phys. **A 346**, 125, (1980); A.E.L. Dieperink, O. Scholten, and F. Iachello, Phys. Rev. Lett. **44**, 1747, (1980).
[35] K. Nomura, N. Shimizu, and T. Otsuka, Phys. Rev. Lett. **101**, 142501 (2008).
[36] J.E. García-Ramos and K. Heyde, Nucl. Phys. **A 825**, 39 (2009).
[37] J.E. García-Ramos, V. Hellemans, and K. Heyde, Phys. Rev. **C 84**, 014331 (2011).
[38] E.A. McCutchan, R.F. Casten, and N.V. Zamfir, Phys. Rev. **C 71**, 061301(R) (2005).
[39] E.A. McCutchan and N.V. Zamfir, Phys. Rev. **C 71**, 054306 (2005).
[40] E.A. McCutchan, R.F. Casten, V. Werner, R. Winkler, R.B. Cakirli, G. Gürdal, X. Liang, and E. Williams, Phys. Rev. **C 78**, 014320 (2008).
[41] K. Nomura, T. Otsuka, R. Rodríguez-Guzmán, L. M. Robledo, and P. Sarriguren, Phys. Rev. **C 83**, 014309 (2011).
[42] K. Nomura, T. Otsuka, R. Rodríguez-Guzmán, L. M. Robledo, P. Sarriguren, P.H. Regan, P.D. Stevenson, and Z. Podolyak, Phys. Rev. **C 83**, 054303 (2011).
[43] K. Nomura, T. Nikšić, T. Otsuka, N. Shimizu, and D. Vretenar, Phys. Rev. **C 84**, 014302 (2011).
[44] K. Nomura, R. Rodríguez-Guzmán, L. M. Robledo, and N. Shimizu, Phys. Rev. **C 86**, 034322 (2012).
[45] K. Nomura, R. Rodríguez-Guzmán, and L. M. Robledo, Phys. Rev. **C 87**, 064313 (2013).
[46] D.D. Warner and R.F. Casten, Phys. Rev. **C 28**, 1798 (1983).
[47] K. Heyde, P. Van Isacker, R.F. Casten and J.L. Wood, Phys. Lett. **B 155**, 303 (1985).
[48] K. Heyde, J. Jolie, J. Moreau, J. Ryckebusch, M. Waroquier, P. Van Duppen, M. Huyse, and J.L. Wood, Nucl. Phys. **A 466**, 189 (1987).
[49] A. Bohr and B. R. Mottelson, *Nuclear Structure, Vol. II*, W. A. Benjamin Inc. Advanced Book Program Reading Massachusetts (1975)
[50] A. Frank, O. Castaños, P. Van Isacker, and E. Padilla, AIP Conf. Proc. **638**, 23 (2002).
[51] A. Frank, P. Van Isacker, and C.E. Vargas, Phys. Rev. **C 69**, 034323 (2004).
[52] A. Frank, P. Van Isacker, and F. Iachello, Phys. Rev. **C73**, 061302(R) (2006).

[53] I.O. Morales, A. Frank, C.E. Vargas, and P. Van Isacker, Phys. Rev. **C78**, 024303 (2008).
[54] L. M. Robledo, R. Rodríguez-Guzmán, and P. Sarriguren, J. Phys. G: Nucl. Part. Phys. **36**, 115104 (2009).
[55] J. Kotila, K. Nomura, L. Guo, N. Shimizu, and T. Otsuka, Phys. Rev. **C85**, 054309 (2012).
[56] J. E. García-Ramos, V. Hellemans, and K. Heyde, AIP Conf. Proc. **1491**, 109 (2012).
[57] P. Van Isacker and Jin-Quan Chen, Phys. Rev. **C 24**, 684 (1981).
[58] K. Heyde, P. Van Isacker, M. Waroquier, and J. Moreau, Phys. Rev. **C 29**, 1420 (1984).
[59] A. Leviatan and M.W. Kirson, Ann. Phys. **201**, 13 (1990).
[60] V. Hellemans, P. Van Isacker, S. De Baerdemacker, and K. Heyde, Nucl. Phys. **A 819**, 11 (2009).
[61] K. Nomura, N. Shimizu, D. Vretenar, T. Niksic, and T. Otsuka, Phys. Rev. Lett. **108**, 132501 (2012).
[62] M.K. Harder, K.T. Tang, and P. Van Isacker, Phys. Lett. **B 405**, 25 (1997).
[63] Th. Hilberath, St. Becker, G. Bollen, H.-J. Kluge, U. Krönert, G. Passler, J. Rikovska, R. Wysse, and the ISOLDE Collaboration, Z. Phys. **A 342**, 1 (1992).